

# Magnetoresistance extremum at the first-order Verwey transition in magnetite ( $\text{Fe}_3\text{O}_4$ )

V. V. Gridin and G. R. Hearne

*Department of Physics, University of the Witwatersrand, Private Bag 3, P.O. Wits 2050, Johannesburg, South Africa*

J. M. Honig

*Department of Chemistry, Purdue University, West Lafayette, Indiana 47907*

(Received 17 October 1995)

A large negative magnetoresistance (MR) sharply peaked at the first-order Verwey transition temperature  $T_V = 119.79 \pm 0.02$  K has been measured in a synthetic single crystal of magnetite  $\text{Fe}_{3(1-\delta)}\text{O}_4$ ,  $\delta = 0.0006$ . At  $H = 7.7$  T the MR extremum exhibited a peak value of  $-17\%$  and a full width at half maximum of  $0.53 \pm 0.08$  K. At the lower and higher ends of the measurement interval 114–126 K encompassing  $T_V$ , negative MR values of 3% and 0.5%, respectively, were obtained at 7.7 T. In applied magnetic fields up to 7.7 T the field-dependent discontinuous entropy change at  $T_V$ ,  $\Delta\sigma_H$ , decreases linearly with respect to the zero-field value  $\Delta\sigma_0$ , according to  $\Delta\sigma_H = \Delta\sigma_0 - k_B|\text{MR}|$ . At  $T_V$ , the associated discontinuous change of the average magnetic moment  $\langle\mu\rangle$  obtained from the MR data was of the order of  $\Delta\mu = 0.1\%$  of  $\langle\mu\rangle$ . This is concordant with the corresponding value obtained in previous magnetization studies. [S0163-1829(96)02123-6]

## I. INTRODUCTION

Since the discovery of the Verwey transition in magnetite,<sup>1</sup> there has been considerable research interest in studying various physical parameters associated with this rather unique order-disorder transition occurring in a strongly correlated electronic system.<sup>2</sup> There have been extensive investigations of electrical transport,<sup>3–8</sup> magnetization,<sup>9,10</sup> Hall effect,<sup>11,12</sup> heat capacity,<sup>13–15</sup> and Seebeck effect<sup>16,17</sup> in the last 50 years of research activity on magnetite, all of which are pertinent to our present study of magnetoresistance.

By contrast, the moderate- to high-magnetic-field regime (2–10 T) study of magnetoresistance (MR) has apparently been attempted only by Feng, Pashley, and Nicolet<sup>8</sup> in their studies to 2.3 T on a polycrystalline thin-film sample. Their study covered a wide temperature interval of 250–100 K; the negative MR data at 2.3 T exhibited a very broad profile with a peak value of  $-7.5\%$  at  $\sim 130$  K.

In this work we report MR measurements in fields up to 7.7 T on a well-characterized synthetic single crystal of  $\text{Fe}_{3(1-\delta)}\text{O}_4$ ,  $\delta = 0.0006$ . Details of the synthesis and characterization may be found in Ref. 15. Our investigation has been conducted in a limited temperature interval of 16 K encompassing the Verwey transition temperature  $T_V = 119.79 \pm 0.02$  K as identified by zero-field conductivity measurements. An attempt has been made to interpret these data in terms of standard thermodynamic considerations to estimate the discontinuous change of both entropy and magnetization at  $T_V$ .

## II. EXPERIMENTAL PROCEDURE AND RESULTS

The MR study was conducted in temperature- and field-controlled regimes in a commercial Janis Cryostat incorporating a 9-T superconducting magnet. A bar of approximate area dimensions  $3 \times 5$  mm<sup>2</sup> and an irregular shape along the other dimension was cut from a fragment of the original

crystal without regard to crystal orientation. X-ray-diffraction measurements performed after the MR study showed that the external field applied perpendicular to the current direction was not along any high-symmetry direction in the cubic lattice. The standard four-probe arrangement was used for current and voltage contacts on the exposed area cut from the original fragment. The 36 AWG copper wires were attached to the exposed face of the sample, after cleaning by abrasion, using commercially available silver paste. This arrangement provided reliable contacts, sufficiently rugged against the possible effects of thermal cycling in subsequent temperature settings. Data were collected in the discrete mode (i.e., at fixed temperatures). Temperature regulation was achieved by means of a Lake-Shore controller, and the superconducting magnet was mostly operated in persistent current mode.

The sample was located between the source of helium exchange gas (vaporizer) and the top of the sample mount to help ensure temperature stability of better than  $\sim 20$  mK over several hours. The temperatures of both locations were regulated by carbon glass resistors (CGR's) mounted in appropriate positions. The temperature of the sample was measured independently by a third calibrated CGR sensor thermally anchored in close proximity to the sample. A conventional current-flipping polarity technique was used to account for possible thermal voltage offsets in our potentiometric measurements. The current (derived from a Lake-Shore source stable to one part in  $10^6$ ) was limited to 30  $\mu\text{A}$  to minimize self-heating effects in the sample having a resistance  $R \sim 100$  m $\Omega$  at  $\sim 124$  K. The following measurement procedure was adopted to collect MR data at discrete temperatures upon cooling in the temperature interval 114–126 K.

(a) The temperature was first stabilized at an initial temperature  $T_i \sim 124$  K to record a zero-field (ZF) datum  $R(T_i, 0)$  for comparison with other experimental runs.

(b) The sample was cooled in ZF to a temperature below 124 K to collect the next datum  $R(T, 0)$ . Resistance values

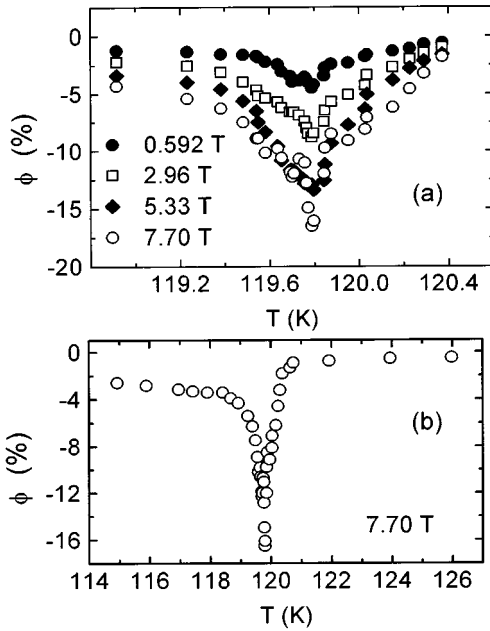


FIG. 1. (a) Magnetoresistance  $\phi = [R(H) - R(0)]/R(0)$  in percent near to the Verwey transition  $T_V$  as a function of applied field  $H$ . (b) Magnetoresistance in the full temperature interval and highest applied field of this study. The FWHM  $\delta T_{1/2} = 0.53 \pm 0.08$  K,  $T_V = 119.79 \pm 0.02$  K and  $\phi^* \equiv \phi(T = T_V) = 0.165$ .

$R(T, H)$  with an experimental reproducibility of  $\sim 0.2\%$  were then acquired at discrete field values  $H$  in the step-ramp sequence 0.5921, 2.9605, 5.3289, and 7.6973 T, with a reproducibility of 10–20 G between the discrete temperature settings. Data at selected temperatures as the field values were lowered from 7.7 T to zero in the same step-ramp sequence were within the experimental reproducibility of the increasing step-ramp  $R(T, H)$  measurements. After reducing the field to zero, a second reading of  $R(T, 0)$  was recorded to verify that no drift had occurred to within  $\sim 20$  mK of the initial temperature setting. An average value of  $R(T, 0)$  was then computed from the prefield and post-field measurements and used to calculate MR, designated as  $\phi = \phi(T, H)$ , according to

$$\phi = \frac{R(T, H) - R(T, 0)}{R(T, 0)}. \quad (1)$$

(c) The sample was then cooled in ZF to another temperature, and the field step-ramping procedure in (b) was repeated to obtain the next set of values for  $\phi(T, H)$ .

Experiments to collect  $R(T, H)$  data at different values of the applied field at several fixed temperature in the interval 126–114 K [sequence (a)–(c) above] were repeated on a daily basis over a period of 14 days to build up a family of MR curves depicted in Fig. 1(a). It may be noted that no field corrections to the CGR temperature sensors were necessary because of the field step-ramping procedure applied at a fixed temperature established under ZF conditions [see procedure (b) in the preceding paragraph] to compute a sequence of  $\phi(T, H)$  values using Eq. (1). We observed no thermal hysteresis upon heating to 124 K from temperatures

below  $T_V$  in zero field. The ZF resistance at 124 K,  $R(T_i, 0)$ , was reproducible to within 0.2% over the 14-day interval of the experiment.

The MR shows a sharp peaked behavior at  $T_V$ ; see Fig. 1. There is a sharp negative peak of  $\sim 17\%$  having a full width at half maximum (FWHM) of  $0.53 \pm 0.08$  K at the highest field of 7.7 T. At the lower and higher ends of the measured temperature interval the MR reduces to negative values of 3% and 0.5%, respectively, at 7.7 T; see Fig. 1(b). The peak MR value, that is,  $\phi(T = T_V)$ , appears to change linearly with increasing field strength; there is no sign of saturation at 7.7 T.

It should be noted that negative MR has previously been reported in magnetite.<sup>8</sup> Feng, Pashley, and Nicolet<sup>8</sup> measured a definite, albeit broad extremum, located near  $T_V$  in their negative MR data on polycrystalline thin-film samples of magnetite in the temperature interval 250 K down to 100 K. At 2.3 T their results show a rather large  $-7.5\%$  extremum at  $\sim 130$  K that diminishes to  $-5\%$  and  $-6\%$  at the higher and lower ends of the temperature interval. The very broad profile obtained by Feng, Pashley, and Nicolet<sup>8</sup> having a FWHM of several K may have been due to the polycrystalline nature of their films and/or the reduced temperature accuracy ( $\sim 0.5$  K) and stability ( $\sim 0.15$  K) of their experimental arrangement. Their resistance data also appear to have been measured at discrete temperatures that differ by  $\sim 5$  K from adjacent points, in contrast to our measurements. It is noteworthy that our MR data exhibit a negative peak profile in a considerably narrower temperature interval ( $\Delta T < 0.6$  K) compared with the data of Ref. 8.

### III. DISCUSSION

We begin with the accepted relation<sup>18</sup> for the resistivity of magnetite that is applicable only very close to  $T_V$ , similar to the temperature range of this study, namely,

$$\rho = \rho_0 \exp\left[\frac{\varepsilon}{k_B T}\right], \quad (2)$$

where  $\varepsilon$  is an activation energy per  $\text{Fe}_3\text{O}_4$  formula unit (or enthalpy, since work is done to activate the carrier transport), corresponding to charge exchange between the  $\text{Fe}^{2+}$  ( $3d^6$ ) and  $\text{Fe}^{3+}$  ( $3d^5$ ) octahedral sites in the unit cell. At the transition temperature the activation energy  $\varepsilon$  is strongly temperature dependent due to the sharp change in Arrhenius slopes at  $T_V$ . Therefore in the vicinity of  $T_V$  we set  $\varepsilon_H \equiv \varepsilon(T, H)$  and we assume that Eq. (2) is still applicable in the analysis of our results. By using the definition of MR in Eq. (1), it is easily shown that

$$1 + \phi = \exp\left[\frac{\varepsilon_H - \varepsilon_0}{k_B T}\right], \quad (3)$$

where  $\varepsilon_0$  is the temperature-dependent activation energy in zero field in the vicinity of  $T_V$ . This expression may be approximated as

$$\phi \approx \frac{(\varepsilon_H - \varepsilon_0)}{k_B T}, \quad (4)$$

given that  $|\phi| \ll 1$  from our MR results. At the first-order transition temperature  $T_V$ , the discontinuous change in enthalpy,

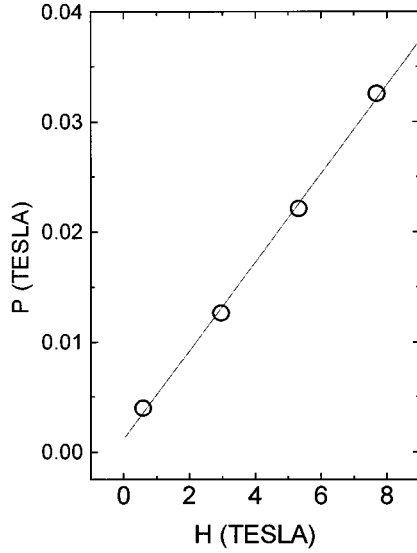


FIG. 2. A plot of  $P \equiv (|\phi^*|k_B\delta T_{1/2})/(gS\mu_B)$  vs applied field  $H$ ; see Eq. (8) in the text. The solid line is a linear least-squares fit of the data. The change in magnetic moment per  $\text{Fe}_3\text{O}_4$  formula unit at  $T_V$  in units of  $\mu_B$ ,  $\Delta\mu = 0.0040 \pm 0.0004$ , is obtained from the slope.

$\Delta\varepsilon = \varepsilon^+ - \varepsilon^-$  (+ and - referring to just above and below  $T_V$ , respectively) may be rewritten in terms of the discontinuous change in entropy  $\Delta\sigma$ , namely,  $\Delta\varepsilon_H = \Delta\sigma_H T_V$ , where the subscript  $H$  refers to the discontinuous change of the thermodynamic variable in the applied field  $H$  at  $T_V$ . The discontinuous change in entropy at  $T_V$  is supposed to lead to a corresponding change in MR,  $\Delta\phi$ , because of the relation in Eq. (4); that is,

$$\Delta\phi \approx \frac{(\Delta\varepsilon_H - \Delta\varepsilon_0)}{k_B T_V} = \frac{(\Delta\sigma_H - \Delta\sigma_0)}{k_B}. \quad (5)$$

By applying the equilibrium condition to small temperature and local-field strength variations at the first-order transition, that is, by setting small variations in the Gibbs energy to zero, it can be shown that<sup>19</sup>

$$(\sigma_H - \sigma_0)\delta T = -H\delta M, \quad (6a)$$

where  $M$  is the macroscopic magnetization per  $\text{Fe}_3\text{O}_4$  formula unit. For two phases, designated phase I and II, in equilibrium at the transition, fluctuations in temperature lead to fluctuations in magnetization. That is,  $\delta M_I = \delta M_{II} + \Delta M$ , where  $\Delta M$  is the discontinuous change in magnetization at  $T_V$  associated with a discontinuous change in entropy  $\Delta\sigma$ ,<sup>15</sup> from which

$$(\Delta\sigma_H - \Delta\sigma_0)\delta T = -H\Delta M. \quad (6b)$$

We approximate the discontinuous change in  $\phi$  at  $T_V$  by  $\Delta\phi \approx \phi(T=T_V) - \phi(T>T_V) \approx \phi(T=T_V)$  from Fig. 1, and denote this as  $\phi^*$ . The change in  $\phi$  at  $T_V$ , Eq. (5), with the aid of Eq. (6b), may then be reformulated in terms of the applied field  $H$ , the magnetization per  $\text{Fe}_4\text{O}_4$  formula unit, and quantities determined from the experimental data in Fig. 1, namely,

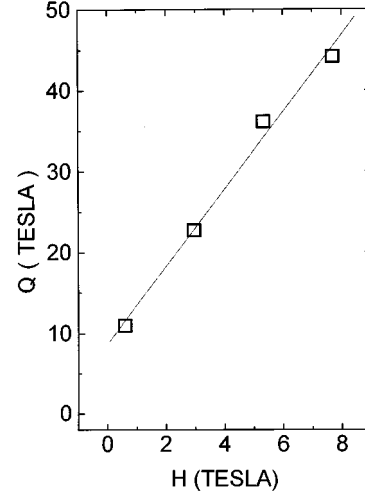


FIG. 3. A plot of  $Q \equiv (|\phi^*|6k_B T_V)/(gS\mu_B)$  vs applied field  $H$ , see Eq. (9) in the text. The solid line represents a linear least-squares fit of the data. The magnetic moment per  $\text{Fe}_3\text{O}_4$  formula unit in units of  $\mu_B$ ,  $\mu = 4.7 \pm 0.5$ , at  $T_V$  is obtained from the slope.

$$|\phi^*| \approx -\frac{\Delta\sigma_H - \Delta\sigma_0}{k_B} \approx \frac{\Delta M}{k_B} \frac{H}{\delta T_{1/2}}, \quad (7)$$

where  $\delta T \equiv \delta T_{1/2}$  is the FWHM (i.e., the temperature interval at  $\phi^*/2$ ) of the MR profile in Fig. 1 for a given value of  $H$ . The macroscopic magnetization  $M$  and magnetic moment  $\mu$  per  $\text{Fe}_3\text{O}_4$  formula unit are related by  $M = gS\mu$ , where  $g=2$  is the Landé factor and  $S=2$  is an effective atomic spin of the cation (Fe) electronic state.<sup>20</sup> Hence a discontinuous change in magnetization is associated with a corresponding change in magnetic moment  $\Delta\mu$ ,  $\Delta M = gS(\Delta\mu)$ , so that Eq. (7) may be rewritten as

$$|\phi^*| = gS \frac{\Delta\mu}{k_B} \frac{H}{\delta T_{1/2}}. \quad (8)$$

When we consider the change in MR at  $T_V$ ,  $\Delta\phi$ , in terms of enthalpy changes at  $T_V$  using Eq. (5), all nonmagnetic contributions are eliminated by taking the difference of the two terms  $\Delta\varepsilon_H - \Delta\varepsilon_0$ . Since the order-disorder transition at  $T_V$  involves the transfer of an electron from an  $\text{Fe}^{2+}$  to  $\text{Fe}^{3+}$  site in the octahedral interstices of each unit cell,<sup>21</sup> the remaining magnetic contribution to the enthalpy change corresponds to the work done in aligning the extra electron in the local field at the “destination”  $\text{Fe}^{3+}$  site. Hence this single-charge exchange event at  $T_V$  in the presence of an external field should involve a magnetic enthalpy change of  $\Delta\varepsilon_H - \Delta\varepsilon_0 = \frac{1}{6} \times M \times H$ . The prefactor of  $\frac{1}{6}$  corresponds to the fractional change of charge occurring at the original  $\text{Fe}^{2+}$  ( $3d^6$ ) site. Using this expression for the magnetic enthalpy change at  $T_V$ , the relation between  $M$  and  $\mu$ , and Eq. (5),  $\Delta\phi$  at  $T_V$  may be expressed as

$$|\phi^*| = \frac{gS\mu H}{6k_B T_V}. \quad (9)$$

We obtain  $\Delta\mu$  at  $T_V$  from experimental data by manipulating Eq. (8) to plot  $P \equiv (|\phi^*|k_B\delta T_{1/2})/(gS\mu_B)$  versus applied field  $H$ , where  $\mu_B$  is the Bohr magneton; we assume

that  $\Delta\mu$  is independent of  $H$ . Hence a plot of  $P$  against  $H$  (see Fig. 2) should have slope  $\Delta\mu$  in units of  $\mu_B$  (using  $g$  and  $S$  equal to 2). For a single-charge-transfer event per  $\text{Fe}_3\text{O}_4$  formula unit at  $T_V$  we obtain  $\Delta\mu=0.004\pm 0.0004\mu_B$  from a linear least-squares fit of the data in Fig. 2. By using Eq. (9) and plotting  $Q\equiv(|\phi^*|6k_B T_V)/(gS\mu_B)$  versus  $H$  (see Fig. 3), from the slope we obtain a value of  $\mu=4.7\pm 0.5\mu_B$  per  $\text{Fe}_3\text{O}_4$  formula unit from a linear least squares fit of the data. This is in reasonable agreement with the accepted value of  $\mu=4.05\mu_B$  per  $\text{Fe}_3\text{O}_4$  formula unit as recently verified again by the magnetization study of Aragón.<sup>10,22</sup> The rather high value of  $\mu=4.7\pm 0.5\mu_B$  may be an indication that the derivation of Eq. (9) is oversimplified. The relative change in the magnetic moment at  $T_V$ ,  $\Delta\mu/\mu\approx 0.1\%$ , is concordant with the results reported in the magnetization studies of Refs. 9 and 10, corroborating most of the assumptions made in this section.

It should be noted that the discontinuous entropy change at  $T_V$  in an applied field decreases linearly with respect to the value in zero field,  $\Delta\sigma_H=\Delta\sigma_0-k_B|\phi^*|$ ; see Eq. (5). Given

that  $\Delta\sigma_0=k_B\ln 2$ ,<sup>15</sup> we find that, at 7.7 T,  $\Delta\sigma_H$  decreases by  $\sim 25\%$  relative to the zero-field value  $\Delta\sigma_0$ . However, the transition temperature  $T_V$  at the highest field decreases by less than  $\sim 0.3$  K relative to the zero-field value  $T_V\approx 119.8$  K. This should be compared with the effect of an adjustable cation deficiency  $\delta$  in  $\text{Fe}_{3(1-\delta)}\text{O}_4$  on the entropy of transition  $\Delta\sigma_0$ .<sup>15</sup> Values tabulated in Ref. 15 demonstrate that  $\Delta\sigma_0$  decreases by  $\sim 25\%$  as the cation deficiency is increased from  $\delta=0.0007$  (similar to the sample used in this work) to  $\delta\sim 0.0017$ , and  $T_V$  exhibits a corresponding decrease of  $\sim 5$  K, in stark contrast to the behavior of  $T_V$  in the presence of an external field.

## ACKNOWLEDGMENTS

The authors wish to thank R. Aragón, J. W. Koenitzer, and P. A. Metcalf for their assistance in the preparation of the sample. This research was supported in part by NSF-DMR Grant No. 92-22986.

<sup>1</sup>E. J. W. Verwey, *Nature (London)* **144**, 327 (1939).

<sup>2</sup>J. M. Honig and J. Spalek, *J. Less-Common Metals* **156**, 423 (1989).

<sup>3</sup>B. A. Calhoun, *Phys. Rev.* **94**, 1577 (1954).

<sup>4</sup>C. A. Domenicali, *Phys. Rev.* **78**, 458 (1950).

<sup>5</sup>V. A. M. Brabers, *Philos. Mag. B* **42**, 429 (1980).

<sup>6</sup>D. Kostopoulos, *Phys. Status Solidi A* **9**, 523 (1972).

<sup>7</sup>P. A. Miles, W. B. Westphal, and A. von Hippel, *Rev. Mod. Phys.* **29**, 279 (1957).

<sup>8</sup>J. S. Feng, R. D. Pashley, and M. A. Nicolet, *J. Phys. C* **8**, 1010 (1975).

<sup>9</sup>S. Unemura and S. Iida, *J. Phys. Soc. Jpn.* **40**, 679 (1976).

<sup>10</sup>R. Aragón, *Phys. Rev. B* **46**, 5328 (1992).

<sup>11</sup>J. M. Lavine, *Phys. Rev.* **114**, 482 (1959).

<sup>12</sup>D. Kostopoulos and A. Theodossiou, *Phys. Status Solidi A* **2**, 73 (1970).

<sup>13</sup>J. P. Shepherd, R. Aragón, J. W. Koenitzer, and J. M. Honig, *Phys. Rev. B* **32**, 1818 (1985).

<sup>14</sup>J. W. Koenitzer, P. H. Keesom, and J. M. Honig, *Phys. Rev. B* **39**, 6231 (1989).

<sup>15</sup>J. P. Shepherd, J. W. Koenitzer, R. Aragón, J. Spalek, and J. M. Honig, *Phys. Rev. B* **43**, 8461 (1991).

<sup>16</sup>J. M. Lavine, *Phys. Rev.* **123**, 1273 (1961).

<sup>17</sup>R. Aragón, J. P. Shepherd, J. W. Koenitzer, D. J. Buttrey, R. J. Rasmussen, and J. M. Honig, *J. Appl. Phys.* **57**, 3221 (1985).

<sup>18</sup>M. Pai and J. M. Honig, *J. Phys. C* **16**, L35 (1983); R. Aragón, R. J. Rasmussen, J. P. Shepherd, J. W. Koenitzer, and J. M. Honig, *J. Magn. Magn. Mater.* **54-57**, 1335 (1986).

<sup>19</sup>J. M. Honig, *Thermodynamics* (Elsevier, Amsterdam, 1982), Chap. 5.

<sup>20</sup>Conventionally in the inverse spinel structure of  $\text{Fe}_3\text{O}_4$  we consider the majority spins of  $\text{Fe}^{3+}$  in tetrahedral and octahedral sites to cancel out. This leaves only  $\text{Fe}^{2+}$  as an effective contribution, with  $S=2$ .

<sup>21</sup>The distribution of  $\text{Fe}^{2+}$  and  $\text{Fe}^{3+}$  ions in octahedral sites changes from dynamic disorder to long-range order as  $T$  is lowered through  $T_V$ . In octahedrally coordinated interstices above  $T_V$  an electron transfers between iron atoms, whereas below  $T_V$  a charge-ordered small polaron state, with local lattice deformations, occurs and sublattices of  $\text{Fe}^{3+}$  ( $3d^5$ ) and  $\text{Fe}^{2+}$  ( $3d^6$ ) may be discerned.

<sup>22</sup>At  $T_V$  the value quoted for the magnetization per unit mass in Ref. 10 is  $\sim 97.7$  emu/g. Therefore the magnetic moment is  $\mu=(97.7 \text{ erg Oe}^{-1} \text{ g}^{-1} \times 231.55 \text{ amu})/(9.27 \times 10^{-21} \text{ erg Oe}^{-1} \times 6.02 \times 10^{23})=4.05\mu_B$  per  $\text{Fe}_3\text{O}_4$  formula unit.